Mack's determination would yield $D_{298.2\ K} = 0.0786\ cm^2\ s^{-1}$, or $D_{303.2\ K} = 0.0810\ cm^2\ s^{-1}$ if we take the exponent for the temperature correction (*13*) as 1.81. This figure differs from the present determination by 6.2%.

From the data presented here the Schmidt numbers for dilute naphthalene–air and naphthalene–hydrogen mixtures are calculated to be 1.805 and 3.65, respectively.

Glossary

a	cross-sectional area for diffusion, cm^2
C	concentration of diffusing species in gas stream leaving diffusion cell, mol cm^{-3}
C_0	concentration of diffusing species at the initial end of the diffusion path, mol cm^{-3}
D	diffusion coefficient, $cm^2\ s^{-1}$
F	gas flow rate, $cm^3\ s^{-1}$
N	flux of diffusing species, mol $cm^{-2}\ s^{-1}$
x	length of diffusion path, cm

Registry No. Naphthalene, 91-20-3; hydrogen, 1333-74-0.

Literature Cited

(1) Winding, C. C.; Cheney, A. J. *Ind. Eng. Chem.* **1948**, *40*, 1067.
(2) Macleod, N.; Cox, M. D.; Todd, R. B. *Chem. Eng. Sci.* **1982**, *17*, 923.
(3) Bar-Ilan, M.; Resnick, W. *Ind. Eng. Chem.* **1957**, *49*, 313.
(4) Hurt, D. M. *Ind. Eng. Chem.* **1943**, *35*, 522.
(5) Caldwell, L. *Appl. Catal.* **1982**, *4*, 13.
(6) Mack, E. *J. Am. Chem. Soc.* **1925**, *47*, 2468.
(7) Landolt-Börnstein. "Zahlenwerte und Funktionen aus Physik, Chemie, Astronomie, Geophysik und Technik"; 6ste Auflage, II Band, 5 Teil, Springer-Verlag: West Berlin, 1969; p 553.
(8) "International Critical Tables"; McGraw-Hill: New York, 1929; Vol. 5, p 63.
(9) Marrero, T. R.; Mason, E. A. *J. Phys. Chem. Ref. Data* **1972**, *1*, 3.
(10) Barker, J. T. *Z. Phys. Chem.* **1910**, *71*, 235.
(11) Bradley, R. S.; Cleasby, T. G. *J. Chem. Soc.* **1953**, 1690.
(12) Skelland, A. H. P. "Diffusional Mass Transfer"; Wiley: New York, 1974; p 118.
(13) Chen, N. H.; Othmer, D. F. *J. Chem. Eng. Data* **1962**, *7*, 37.

Received for review March 22, 1983. Accepted August 1, 1983.

Acridine Orange Association Equilibrium in Aqueous Solution

Lucia Costantino, Gennaro Guarino, Ornella Ortona, and Vincenzo Vitagliano*

Instituto Chimico Università di Napoli, Naples, Italy

An accurate set of absorption spectra in the visible region has been collected for acridine orange (AO) hydrochloride in aqueous solution at various temperatures and concentrations. The limiting extinction spectra of monomer, dimer, and associated dye species were computed from the experimental data. The free energy, enthalpy, and entropy of dye dimerization have also been computed.

Introduction

Acridine orange (AO) behavior in aqueous solution and its interaction with synthetic and biological polyelectrolytes have been the subject of a very wide literature for 30 years (*1*).

The reason for the interest in AO and similar dyes is mainly connected with their ability to interact with genetic material (*2*, *3*); the similarity of these molecules to several antibiotics, such as daunomycin or actinomycin (*4*), makes them interesting model systems for studying a variety of bio- and physicochemical problems.

AO is a cationic dye, it is protonated at a pH lower than 10–10.5, and its spectrum does not agree with Beer's law. Figure 1 shows the extinction spectra in the visible region of acridine orange hydrochloride in aqueous solution, in the concentration range 10^{-5}–10^{-1} mol/L.

The absorption spectrum of dilute AO, having a maximum at 492 nm (α band), is gradually substituted by a new spectrum with a maximum at 465 nm (β band). In the concentration range below (4–5) × 10^{-5} mol/L an isosbestic point is observed at 471.5 nm.

At higher concentrations the 465-nm band is substituted by a third band (γ band) with a maximum at 450 nm and the isosbestic point disappears.

Such a behavior, characteristic of all metachromatic dyes (acridine derivatives, methylene blue, crystal violet, cyanine dyes, etc.), has been interpreted as due to the association of dye molecules in solution (*1*, *5*).

We have recently studied the association for several *N*-alkyl derivatives of acridine orange and computed the dimerization constants and other thermodynamic properties to compare them with those of AO available in the literature (*6*, *7*).

At this point we thought it convenient to collect a new set of experimental absorption data on AO aqueous solutions in the full range of possible dye concentrations and decided to treat them like those of the other acridine dyes, in order to have a full set of self-consistent thermodynamic data, including the first molecule of the series.

The results discussed in the following were obtained from the analysis of about 200 spectra taken at various concentrations and temperatures.

The association, or stacking, of dye molecules in solution, promoted by the π-electron interactions of aromatic rings, can be described as a set of multiple equilibria of the following type:

$$D + D = D_2 \quad (1)$$

$$D_2 + D = D_3 \quad (2)$$

...

$$D_{n-1} + D = D_n \quad (3)$$

It may be assumed that dye molecules stack in a sandwichlike pile. The α absorption band was attributed to the dye in its monomeric form, the β band to the dimer dye, and the γ band to dye in a higher associated form.

The observed spectral changes have also been predicted theoretically for an association according to this model (*8*, *9*).

The equilibrium constants for the associations 1–3 are given by the following expressions:

$$[D_2] = K_{12}[D]^2 \quad (4)$$

$$[D_3] = K_{12}K_{23}[D]^3 \quad (5)$$

...

$$[D_n] = K_{12}K_{23}...K_{n-1,n}[D]^n \quad (6)$$

0021-9568/84/1729-0062$01.50/0

The total dye concentration in terms of monomer species is

$$C = \sum_{1}^{\infty} n[D_n] \quad (7)$$

and the fraction of dye in the n-th associated form

$$\alpha_n = n[D_n]/C \quad (8)$$

If we assume that the $K_{i-1,i}$ constants differ from each other only because of the electrostatic energy of the growing pile and assume a "medium" electrostatic repulsion effect among charged molecules in the n-mer, each association constant is related to the dimerization constant K_{12} by the expression (*10*)

$$K_{n-1,n} = K_{12} \exp[-q\sum_{2}^{n-1} 1/(n-1)] \quad (9)$$

where

$$q = \epsilon^2/kaT\sigma \quad (10)$$

ϵ being the monomeric dye charge, k the Boltzmann constant, T the absolute temperature, a the average distance between stacked dye molecules, and σ the effective dielectric constant around the charged molecules (at 20 °C, $q = 5.7 \times 10^{-6}/a\sigma$).

Experimental Section

Acridine orange (Merk für Mikroscopie) was purified as described in a previous paper (*11*).

Spectrophotometric Measurements. All solutions for spectrophotometry were prepared by weighing. Several stock AO solutions were made from solid dye and the extinction at $C = 10^{-5}$ mol/L was checked by dilution; the extinction value $E = 55000$, found in the past (*12*), was confirmed. Concentration was always computed from weight data by using the water density at 20 °C. All solutions were made in the presence of 0.001 M HCl in order to secure, at least in dilute AO systems, the constancy of activity coefficients. Spectrophotometric cells with a thickness range from 10 to 10^{-3} cm were used.

Treatment of Data

Assumptions. We assumed, as in the previous papers, that the α band (extinction coefficients E_1) belongs to the dye in monomeric form, the β band (E_2) to the dimer dye, and the γ band (E_3) to any associated dye species higher than dimer.

E_1 Spectra. Limiting extinction coefficients for the monomer species were obtained for a set of wavelengths ranging between 530 and 420 nm by extrapolation of experimental data at infinite dye dilution according to the expression

$$E = E_1 + aC + bC^2 + \ldots \text{ (at each wavelength)} \quad (11)$$

Figure 2A is a graph of eq 11 at two characteristic wavelengths, the maximum of monomer dye (492 nm) and the isosbestic point corresponding to equilibrium 1; this point was assumed at the wavelength where $a = 0$ (eq 11), 471.5 nm. Some numerical extinction values are given in Table I.

Equilibrium Constant K_{12}. The dimerization constant K_{12} was computed by assuming an arbitrary, although reasonable, value for E_2 at 492 nm and computing the fraction of monomeric dye with the expression

$$\alpha_1 = \frac{E - E_2}{E_1 - E_2} \quad (12)$$

$$K_{12}^* = \frac{1 - \alpha_1}{2\alpha_1^2 C} \quad (13)$$

where C is the stoichiometric concentration of AO expressed in terms of monomer species. Equation 12 was applied only in the concentration range 10^{-5}–10^{-4} mol/L for a set of assumed values of E_2. K_{12}^* varies almost linearly with concentration and its limit value at infinite dilution was obtained by graphical extrapolation (see Figure 3A). The limiting value K_{12} does not vary much with E_2. From the graphs of Figure 3A we obtained

$$K_{12} = 8500 + 0.323E_2 \quad (14)$$

The final K_{12} choice is discussed below.

E_3 Spectra. The limiting absorption of associated dye, E_3, was obtained by extrapolation of experimental extinction data

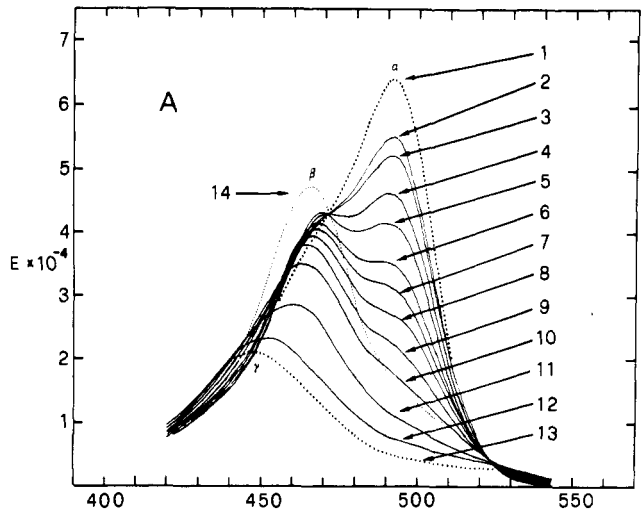

Figure 1. Extinction coefficient spectra of acridine orange in aqueous 0.001 M HCl solution at 20 °C: (1) limiting extinction of monomer dye; (2–12) dye concentrations 10^{-5}, 1.48×10^{-5}, 3.09×10^{-5}, 5.10×10^{-5}, 10^{-4}, 1.56×10^{-4}, 2.78×10^{-4}, 6.25×10^{-4}, 1.6×10^{-3}, 10^{-2}, and 10^{-1} mol/L, respectively; (13) limiting extinction of associated dye; (14) computed extinction of dimer dye.

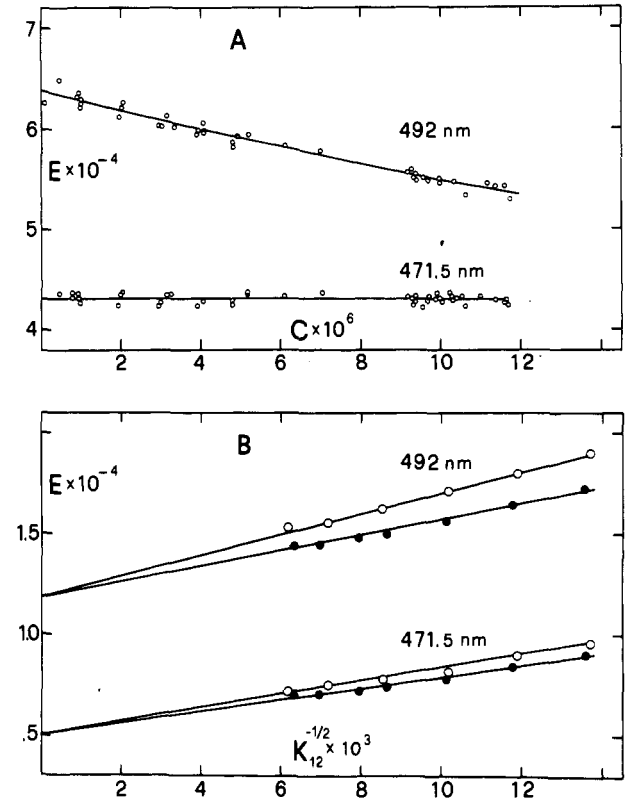

Figure 2. A: Examples of extrapolation of experimental extinctions at infinite dilution to obtain the limiting monomer dye extinction, E_1 (eq 11). 492 nm, maximum absorption of monomer dye; 471.5 nm, isosbestic point of equilibrium 2D = D_2. B: Examples of extrapolation of experimental extinctions as a function of $K_{12}^{-1/2}$ to obtain the associated dye extinctions, E_3; (○) dye concentration, 0.0787 mol/L, (●) dye concentration, 0.0980 mol/L.

Table I. Limiting Extinction Coefficients of Monomer Dimer and Associated Acridine Orange[a]

wavelength, nm	E_1	E_2	E_3	E_2 from E_{12}[b]	
540	400				
530	1 500				
525	3 500				
520	7 000				
515	13 300	8 500	2 800	7 400	
510	22 400	9 700	3 200	9 800	
505	38 900	11 000	3 600	12 500	
500	53 800	13 000	4 100	14 500	
495	62 200	15 400	4 600	16 000	
492	63 800	17 000	5 000	17 000	maximum of monomer dye
490	63 400	18 000	5 300	18 500	
485	58 800	21 500	6 500	23 500	
480	52 000	28 500	8 000	30 000	
475	46 200	37 500	10 200	37 800	
473	44 500	41 000	11 100	41 000	
471.5	43 100	43 100	11 911	43 100	isosbestic point: $2D = D_2$
470	41 900	45 500	12 600	45 000	
468	40 500	46 500	13 600	52 000	
465	38 000	47 000	15 000	52 000	maximum of dimer dye
460	33 400	44 000	17 500	49 400	
455	28 000	38 000	19 700		
450	22 600	30 000	21 000		maximum of associated dye
445	18 500		20 800		
440	15 000		19 000		
430	11 000		14 200		
420	9 000		9 500		

[a] The standard deviation of E_1 is ±150; the standard deviation of E_3 is ±300. The E_2 extinctions were chosen as best-fitting parameters. [b] Obtained from the E_{12} extinctions (see eq 18-20).

Table II. Computed Distribution of Dye among the Various Fractions at 20 °C[a]

C, mol/L	α_1	α_2	α_3	α_4	α_5	α_6	α_7
1.0×10^{-5}	0.8106	0.1840	0.0054	0.0000			
2.5×10^{-5}	0.6681	0.3125	0.0190	0.0003	0.0000		
1.0×10^{-4}	0.4218	0.4982	0.0767	0.0033	0.0000		
4.0×10^{-4}	0.2255	0.5694	0.1874	0.0171	0.0006	0.0000	
0.001111	0.1314	0.5374	0.2864	0.0422	0.0024	0.0001	0.0000
0.002500	0.0826	0.4770	0.3592	0.0749	0.0061	0.0002	0.0000
0.01000	0.0351	0.3445	0.4410	0.1563	0.0216	0.0014	0.0000
0.06250	0.0103	0.1860	0.4373	0.2846	0.0724	0.0088	0.0006
0.1000	0.0074	0.1544	0.4184	0.3139	0.0920	0.0129	0.0010

[a] $K_{12} = 14000$; $q = 3.5$.

of the most concentrated solutions. As suggested by Robinson et al. (*10*), the absorption spectra of highly concentrated solutions were measured as a function of temperature and extinction coefficients were plotted as a function of $K_{12}^{-1/2}$; linear graphs are obtained, the extrapolated values at $K_{12}^{-1/2} \rightarrow 0$ being the E_3 values. These values were found independent of the E_2 choice made for computing K_{12}; furthermore, the same extrapolated values were obtained, within the experimental error, from solutions at different concentrations (see Figure 2B). Actually, the determination of E_1 and E_3 extinction coefficients turns out to be independent of any arbitrary assumptions for treating experimental data.

Choice of E_2 and of K_{12}. Such a choice was made by computing various α_n distributions (from eq 8 and 9) for various K_{12} and q values (see Table II). The extinction coefficients were then computed according to the expression

$$E = E_1\alpha_1 + E_2\alpha_2 + E_3\sum_3^\infty \alpha_n \qquad (15)$$

and compared with the experimental data, in the wavelength range 450–510 nm; various E_2 values were used at each wavelength; at 492 nm the E_2 values given by eq 14 were used for each K_{12} value.

The K_{12}, q, and $(E_2)_\lambda$ set was chosen, which gave the best fitting with the experimental data. A sample of such a fitting is given in Figure 4, where experimental data and computed values have been drawn for $\lambda = 492$ nm and $\lambda = 471.5$ nm as a function of $1/C^{1/2}$.

Table III. Thermodynamic Parameters of Acridine Orange Dimerization in Aqueous Solution[a]

K_{12}[b]	ΔH_{12}	ΔF_{12}[b]	ΔS_{12}	ΔS_u	ref
8 500		−22 000			*12*
22 000	−35 000	−24 400	−36.2	−2.8	*13*
13 000		−23 100			*14*
12 400	−37 800	−23 000	−50.5	−17.0	*10*
14 000	−30 800	−23 300	−25.7	+7.7	our data

[a] Dimerization constant in L/mol; enthalpy and free energy of dimerization (eq 1) in joules; entropy of dimerization in J/K; ΔS_u = unitarian entropy of dimerization. [b] Data at 20 °C.

The average standard deviation between experimental and computed extinctions is of the order of 400–600 extinction units for all the explored wavelength set. The q value was found to be 3.5; some uncertainty appears on the dimerization constant; in fact, K_{12} values between 11 000 and 15 000 L/mol give the same best-fitting results. An alternative approach to the problem enabled us to choose the final values of K_{12} and $(E_2)_\lambda$ given in Tables I and III ($K_{12} = 14000$ and $(E_2)_{492} = 17000$).

Possible Alternative Determination of E_2. It is possible to eliminate the associated-species contribution to the experimental E by using the extinction data at the isosbestic point (Figure 4B); in fact, the expression

$$(E - E_1)/(E_3 - E_1) = \sum_3^\infty \alpha_n = \alpha_A \text{ (at } \lambda = 471.5 \text{ nm)} \qquad (16)$$

corresponds to the fraction of associated dye higher than dimer.

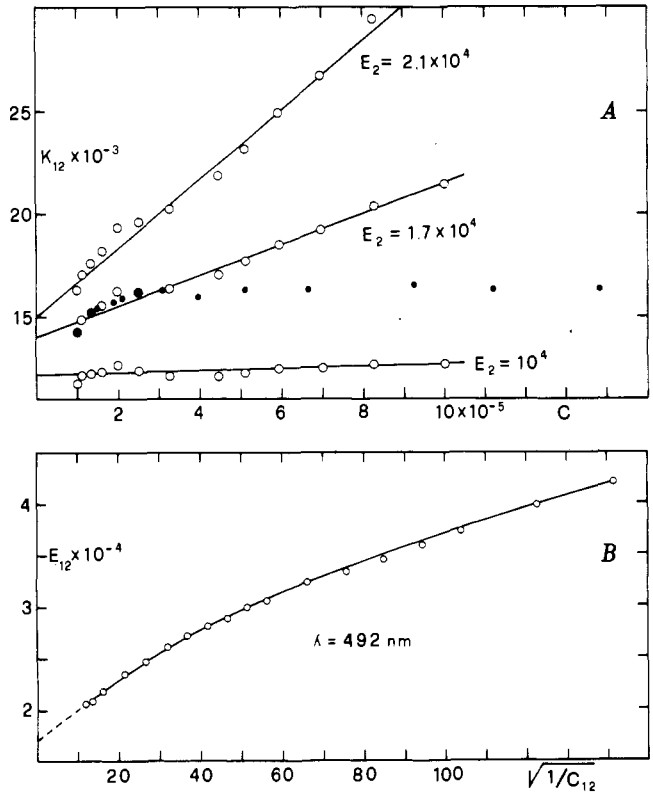

Figure 3. A: Dimerization constant of acridine orange at 20 °C (eq 13) as a function of dye concentration for various dimer extinctions E_2; (●) dimerization constant computed by using the E_{12} values (eq 18). B: Plot of the E_{12} values (eq 18) at 492 nm as a function of the square root of concentration C_{12} of monomer + dimer (eq 19). Extrapolation to obtain E_2.

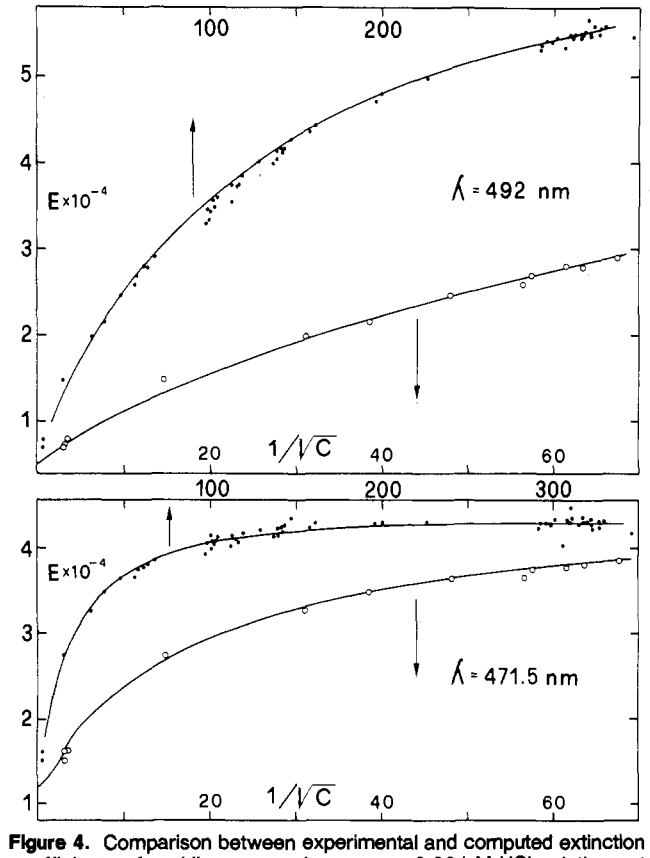

Figure 4. Comparison between experimental and computed extinction coefficients of acridine orange in aqueous 0.001 M HCl solutions at 20 °C and at two wavelengths. C = dye concentration in mol/L.

The contribution to the absorption due only to monomer and dimer is, at any wavelength

$$(E - E_3\alpha_A)C = A_{12} \quad (17)$$

and the corresponding extinction

$$E_{12} = A_{12}/C_{12} = (E - E_3\alpha_A)/(1 - \alpha_A) \quad (18)$$

where

$$C_{12} = (\alpha_1 + \alpha_2)C = (1 - \alpha_A)C \quad (19)$$

is the concentration of monomer + dimer dye.

The E_{12} data extrapolate at $C_{12} \rightarrow \infty$ according to the expression

$$E_{12} = E_2 + \frac{E_1 - E_2}{(2K_{12})^{1/2}}(1/C_{12})^{1/2} + \ldots \quad (20)$$

A graph of E_{12} as a function of $(1/C_{12})^{1/2}$ at 492 nm is shown in Figure 3B; it extrapolates almost linearly at E_2 = 17000. By using E_{12}, E_2, and C_{12} in eq 12 and 13 we computed a new set of K_{12} constants; such a set is shown in Figure 3A for λ = 492 nm (black circles).

On the basis of these results the value E_2 = 17000 at 492 nm for the dimer extinction and the corresponding K_{12} = 14000 L/mol were finally selected. It may be added that the E_2 values obtained according to this treatment are in very good agreement with those obtained from the best fitting of experimental data, as discussed previously, in the λ range 470–520 nm. Some discrepancies appear out of this wavelength range (see Table I). Table II shows the distribution among the various dye species computed through eq 8–10 by using K_{12} = 14000 and q = 3.5.

***Dimerization Enthalpy*, ΔH_{12}.** The dimerization enthalpy was obtained by measuring the absorption spectra of a set of solutions, with concentrations ranging from 10^{-5} to 10^{-4} mol/L, as a function of temperature. The van't Hoff equation was applied to the experimental K_{12}* measured at each temperature and the ΔH_{12}* plotted as a function of dye concentration. The limiting value at $C \rightarrow 0$ was found:

$$\Delta H_{12} = -30800 \pm 2300 \text{ J} \quad (21)$$

No correction for the density change with temperature was applied to the solutions concentration. Since the solutions density at 20 °C is approximately 1.000, the ΔH_{12} given in eq 21 is the dye dimerization enthalpy in the *molal* reference scale.

Discussion

Some authors have already made valuable studies of the acridine orange association equilibrium in aqueous solution (*10*, *13*, *14*); however, only Robinson et al. (*10*) treated the experimental data by accounting also for the presence of aggregates higher than dimers.

The results obtained by these authors are collected in Table III and compared with our present results. As it can be seen the dimerization constants measured by Lamm and Neville (*14*) and by Robinson et al. (*10*) are in good agreement with our results. On the other hand, the old Zanker data (*13*) and those previously obtained in our laboratory (*12*) disagree to some extent. This is most probably due to an incorrect evaluation of the limiting extinctions used for computing the degrees of dimerization. A possible source of errors, in solutions at concentration lower than 10^{-5} mol/L, must be found in the increasing effect of dye adsorption on containers and cell walls. We believe that our present extinction data are very accurate; furthermore, they were obtained from the extrapolation of a quite large number of experimental data and they seem to be in good agreement with those of ref *10* and *14*, although these authors report only graphs of their extinction spectra.

Finally, our measured dimerization enthalpy, ΔH_{12}, is slightly lower than those previously reported; our value leads to computation of a smaller dimerization entropy and a more positive

unitarian entropy of dimerization (entropy corrected for the effect of the disappearance of a solute mole on dimerization) (*15*).

This result is in good agreement with our previous results on acridine orange *N*-alkyl derivatives (*6*, *7*) and is in favor of our suggestion, also proposed by other authors (*16*–*20*), on the dominant contribution of hydrophobic interactions to the association of these dyes in aqueous solution.

Registry No. Acridine orange hydrochloride, 65-61-2.

Literature Cited

(1) Vitagliano, V. In "Aggregation Processes in Solution"; Wyn-Jones, E., Gormally, J., Eds.; Elsevier: Amsterdam, 1983; pp 271–308.
(2) Schreiber, J. P.; Daune, M. P. *J. Mol. Biol.* **1974**, *83*, 487–501.
(3) Lerman, L. S. *J. Mol. Biol.* **1961**, *3*, 18–30.
(4) Crescenzi, V.; Quadrifoglio, F. In "Polyelectrolytes and Their Applications"; Rembaum, A., Sélégny, E., Eds.; Reidel: Dordrecht, Holland, 1975; pp 217–30.
(5) Michaelis, L. *J. Phys. Chem.* **1950**, *54*, 1–17.
(6) Vitagliano, V.; Costantino, L.; Staiano, N.; Ortona, O.; Wurzburger, S. *Adv. Mol. Relaxation Interact. Processes* **1978**, *12*, 251–63.
(7) Costantino, L.; Ortona, O.; Sartorio, R.; Silvestri, L.; Vitagliano, V. *Adv. Mol. Relaxation Interact. Processes* **1981**, *20*, 191–8.
(8) Mason, S. F. *J. Soc. Dyers Colour.* **1968**, 604–12.
(9) Lami, A.; Del Re, G. *Chem. Phys.* **1978**, *28*, 155–65.
(10) Robinson, B. H.; Löffler, A.; Schwarz, G. *J. Chem. Soc., Faraday Trans. 1* **1973**, *69*, 56–69.
(11) Vitagliano, V.; Costantino, L.; Zagari, A. *J. Phys. Chem.* **1973**, *77*, 204–10.
(12) Caramazza, R.; Costantino, L.; Vitagliano, V. *Ric. Sci., Parte 2: Sez. A* **1964**, *34*, 67–73.
(13) Zanker, V. *Z. Phys. Chem.* **1952**, *199*, 225–58.
(14) Lamm, M. E.; Neville, D. M., Jr. *J. Phys. Chem.* **1965**, *69*, 3872–7.
(15) Kauzmann, W. *Adv. Protein Chem.* **1959**, *14*, 1–63.
(16) Mukerjee, P.; Ghosh, A. K. *J. Am. Chem. Soc.* **1970**, *92*, 6419–24.
(17) Haugen, G. R.; Hardwick, E. R. *J. Phys. Chem.* **1963**, *67*, 725–31.
(18) Uedaira, Ha.; Uedaira, Hi. *Kolloid Z.* **1964**, *194*, 148–50.
(19) Blandamer, M. J.; Brivati, J. A.; Fox, M. F.; Symons, M. C. R.; Verma, G. S. P. *Trans. Faraday Soc.* **1967**, *63*, 1850–7.
(20) Rohatgi, K. K.; Mukhopadhyay, A. K. *Chem. Phys. Lett.* **1971**, *12*, 259–60.

Received for review January 11, 1983. Accepted July 26, 1983. This research was supported by the Italian C.N.R. and by the M.P.I.

Composition of Ternary Systems Comprising Water, *n*-Butyl or Isobutyl Alcohol, and One of the Four Mineral Acids $HClO_4$, HNO_3, HCl or H_2SO_4

I. Molnár-Perl,* A. Kisfaludi, and M. Pintér-Szakács

Institute of Inorganic and Analytical Chemistry, L. Eötvös University, Budapest, Hungary

Phase boundary data of the following ternary systems are presented: water–*n*-butyl alcohol–perchloric acid; water–isobutyl alcohol–perchloric acid; water–*n*-butyl alcohol–nitric acid; water–*n*-butyl alcohol–hydrochloric acid; water–isobutyl alcohol–hydrochloric acid; water–*n*-butyl alcohol–sulfuric acid; water–isobutyl alcohol–sulfuric acid; water–*n*-butyl alcohol–phosphoric acid. A well-defined correlation is suggested between the composition and the extent of the homogeneous region and the mineral acids contained in it.

Introduction

The investigation was undertaken to provide some basic analytical information concerning the various butyl alcohol–water–mineral acid systems used in esterification of fatty acids with butyl alcohol in solutions containing different amounts of water.

In the preceding papers (*1*–*7*), the liquid equilibria of ternary systems of water–a butyl alcohol isomer–a mineral acid were investigated for practical extraction purposes. Reburn and Shearer (*1*) determined the parameters of the water–isobutyl alcohol, isoamyl alcohol–HBr, HI, HCl systems, the nonaqueous phases of which are good electric conductors. Legge and Morieson (*2*) studied various butyl alcohol–water–acetic acid systems used in the countercurrent distribution of peptides and proteins. Further observations were reported on the optimal

Table I. Phase Boundary Data of Water-Perchloric Acid–*n*-Butyl Alcohol System

	[component], mol %		
no.[a]	water	perchloric acid	*n*-butyl alcohol
1	98.08	0	1.92
2	94.45	2.58	2.97
3	93.91	2.80	3.29
4	91.45	3.37	5.18
5	91.41	3.78	6.81
6	90.42	3.47	6.11
7	88.92	3.63	7.45
8	87.62	3.63	8.75
9	86.73	3.69	9.58
10	85.67	3.75	10.59
11	85.07	3.74	11.19
12	84.64	3.76	11.73
13	82.66	3.89	13.46
14	80.51	3.84	15.65
15	79.75	3.84	16.41
16	79.14	3.83	17.05
17	78.22	3.71	18.07
18	75.94	3.71	20.35
19	73.26	3.50	23.47
20	68.68	3.28	28.04
21	65.04	3.04	31.92
22	60.01	2.36	37.63
23	53.24	2.09	44.67
24	50.06	1.36	48.58
25	47.43	0	52.57

[a] Number of measurement (in this table and in all following tables).

0021-9568/84/1729-0066$01.50/0